

1 **Lattice parameter of ferrite in silicon cast irons**

2

3 Marcos Lopez^{a,b}, Moukrane Dehmas^a, Jacques Lacaze^a

4

5 a. CIRIMAT, Université de Toulouse, 31030 Toulouse, France

6

7 b. INTEMA, UNMdP – CONICET, Mar del Plata, Argentina

8

9 **corresponding author:** Jacques Lacaze Jacques.lacaze@ensiacet.fr

10 **Abstract**

11 While the density of materials is important for their mechanical and service properties, it is
12 striking that so little is known in the case of silicon cast irons, which are essentially Fe-C-Si
13 alloys with graphite precipitates in an iron-rich matrix. In this work, a review of literature data
14 was used to establish an expression for the lattice parameter of ferrite based on that of pure
15 iron, to which were added the individual effects of carbon, silicon, manganese, phosphorus
16 and copper. The expression thus obtained is valid for a homogeneous material, and a
17 correction is proposed to take account of the presence of graphite in Fe-C-Si ferritic alloys.

18 Next, the ferrite lattice parameter of a series of 12 alloys containing carbon between 1.0 and
19 4.1 wt.%, silicon between 0.5 and 4.3 wt.%, up to 0.7 wt.% Mn and up to 0.9 wt.% Cu, was
20 measured by XRD from room temperature to a temperature of 1150°C. These recordings
21 showed that the mirror polishing used to prepare the samples resulted in surface alteration and
22 a significant overestimation of the ferrite lattice parameter for temperatures below 500°C. We
23 therefore carried out high-energy XRD at room temperature, which was free of any surface
24 effects and validated our analysis. Valid measurements at room temperature and XRD values
25 obtained at temperatures above 500°C were then successfully compared with the predictions
26 given by the proposed expression for the lattice parameter of ferrite as a function of
27 temperature and alloying elements. This work provides the necessary information to calculate
28 the theoretical density of ferritic cast irons.

29

30 **Keywords:** ferrite, lattice parameter, cast iron, XRD, HEXRD

31

32 **1. Introduction**

33 Knowledge of the density of cast irons is a prerequisite for the improvement of their casting
34 process and service properties. Silicon cast irons are composite materials made of graphite
35 precipitates embedded in a Fe-rich matrix that is austenite at high temperature and ferrite or
36 pearlite at low temperature. In fact, the graphite fraction varies according to casting
37 conditions, in particular the carbon supersaturation of austenite at high temperatures and the
38 amount of pearlite at intermediate and low temperatures, generating disparities in thermal
39 expansion and density values. Furthermore, even for a given matrix microstructure, direct
40 estimates of the room-temperature density of cast irons show wide dispersion due to the
41 frequent presence of defects such as micro-porosity. As part of a study dedicated at
42 characterizing the effect of temperature on the density change of silicon cast irons by
43 dilatometry, it appeared necessary to have an independent evaluation of the lattice parameters
44 of the involved phases to calculate their theoretical density. The present work is focused on
45 ferrite and reports firstly on a review of literature information and then on experimental
46 results on alloys containing up to 4.3 wt.% silicon.

47

48 **2. Review of literature information**

49 **2.1 Pure Fe**

50 In a review appeared in 1991 and devoted to the thermomechanical properties of iron-carbon
51 alloys, Jablonka *et al.* listed 11 papers dealing with the effect of temperature on the lattice
52 parameter of pure Fe [1]. They noticed that all data for Fe- α were very close to each other but
53 those from Esser and Müller (referenced by Jablonka *et al.*) that they excluded during their
54 further evaluation. Results by Lihl and Ebel [2], Basinski *et al.* [3], Gorton *et al.* [4], Ridley
55 and Stuart [5], as well as the more recent results by Seki and Nagata [6] are plotted in Fig. 1-
56 a. Note that the first two series of data were given in kX units and have been converted to
57 Ångstrom by multiplying with the coefficient 1.00202 selected by Bragg and Armstrong-
58 Wood [7]. All these data were tabulated in the original works but that by Ridley and Stuart [5]
59 who plotted results for two pure iron samples, one with spectrographic and the other with
60 electrolytic designations. These results lied on the same curve, and those for the
61 spectrographic material have been picked up from the figure produced by the authors for
62 plotting the graph in Fig. 1-a. All data are very close to each other from room temperature up
63 to 500°C, apart for some scatter at room temperature. Above 500°C, the results by Gorton *et*

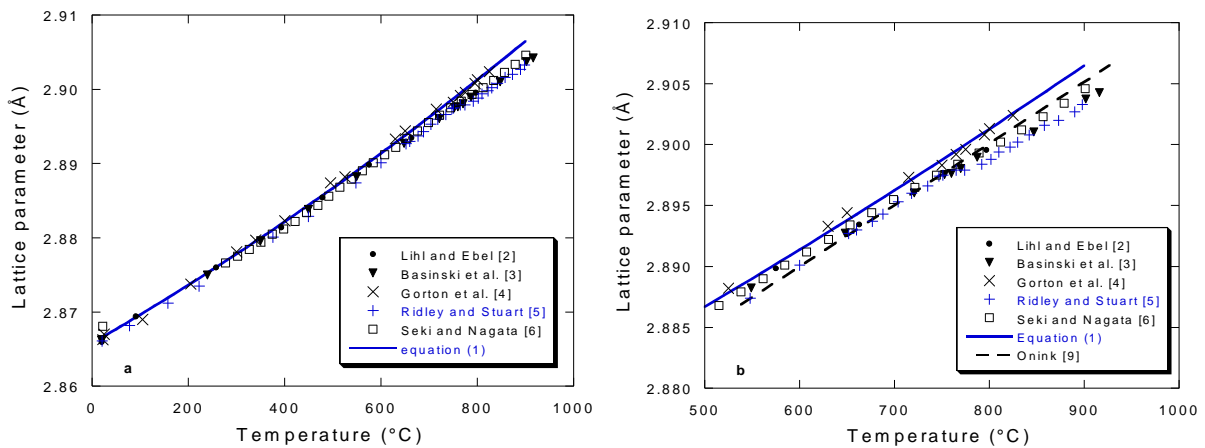
64 *al.* [4] assume slightly higher values while the others remain in good agreement between each
 65 other.

66 Ridley and Stuart [5] mentioned that Esser and Müller reported an anomaly at the Curie
 67 temperature of Fe- α as occurs for nickel. This anomaly was not seen by Basinski *et al.* [3]
 68 while it was considered by Gorton *et al.* [4]. These latter authors fitted their results with the
 69 following equation (\AA):

$$70 \quad a_{Fe-\alpha} = 2.8658 + 3.747 \cdot 10^{-5} \cdot T_C + 8.59 \cdot 10^{-9} \cdot (T_C)^2 \quad (1)$$

71 where T_C is the temperature expressed in Celsius. The lattice parameter at 20°C would thus be
 72 2.8666 \AA that is very close to the value of 2.8664 \AA that is generally accepted for room
 73 temperature, e.g. by Lee and Lee [8].

74



75

76 Figure 1. Lattice parameter of Fe- α between room temperature to 900°C (a) and between
 77 500°C and 900°C (b). Symbols represent data from literature as indicated in the captions. The
 78 solid line corresponds to equation (1) and the dashed line in b was drawn according to Onink
 79 *et al.* [9].

80

81 Gorton *et al.* [4] noticed that their equation should be exclusive of the magnetic
 82 transformation range 715°C to 825°C, but in fact this transformation showed little effect in
 83 their case. However, the enlargement in Fig. 1b for the high temperature range shows that the
 84 effect of the magnetic transformation is more significant in works by Seki and Nagata [6],
 85 Ridley and Stuart [5] and Lihl and Ebel [2]. The magnetic anomaly is clearly seen in a
 86 temperature interval of about 35°C around the Curie temperature (770°C) where it relates to a

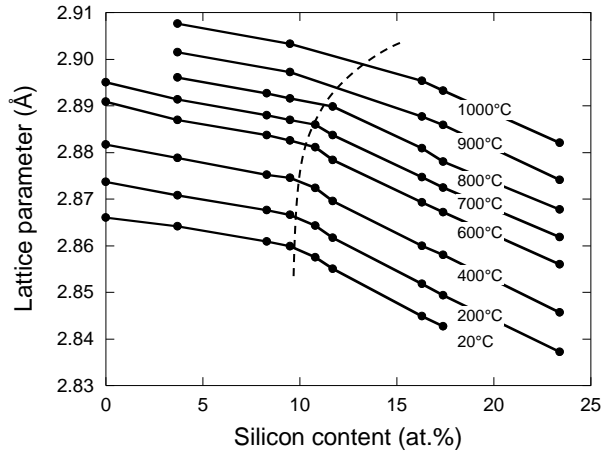
87 decrease in the mean linear thermal expansion coefficient on heating through the Curie
88 temperature. In addition, Onink *et al.* [9] published results on Fe-C alloys including also pure
89 Fe. Considering that the carbon content in Fe- α is negligible, they averaged their data on pure
90 Fe and three of the four Fe-C alloys they investigated to give an equation describing the
91 ferrite lattice parameter between 600°C and 900°C, not even mentioning the possible effect of
92 the magnetic transformation. Their equation has been plotted in Fig. 1b where it is seen that it
93 underestimates the lattice parameter below the magnetic transition and overestimates it above
94 the transition, and this is what is also seen in the Fig. 6 of Onink *et al.* [9].

95

96 **2.2 Role of carbon, silicon and other alloying elements**

97 Many works on steels assume that the solubility of carbon in Fe- α is so low that this element
98 will not affect the lattice parameter. However, the upper temperature for ferrite in high silicon
99 cast irons is quite high and may be associated with an increase of the carbon solubility. In this
100 line, the work by Fasiska and Wagenblast [10] is worth consideration. These authors
101 evaluated experimentally that carbon dilates the ferrite lattice by an amount of $8.4 \cdot 10^{-3}$ Å/at.%
102 independent of temperature.

103 The effect of silicon on Fe- α has been investigated since a long time as Fe-Si alloys are the
104 base for soft magnetic steels. Studies have in particular focused on the determination of the
105 boundaries between the disordered bcc-A2 and its two ordered variants, B2 (based on FeSi
106 compound) and DO₃ (based on Fe₃Si). Amongst the many available studies, the one by Lihl
107 and Ebel [2] is worth of mention for the extensive and tabulated results that are reproduced in
108 Fig. 2. These results were given in kX and were converted to Ångström as already indicated.
109 Polishchuk and Selisskiy [11] have provided results for temperature up to 1200°C that appear
110 quite similar but were not given as a table as did Lihl and Ebel. Fig. 2 evidences that silicon
111 decreases the lattice parameter of Fe- α , and this effect is larger for the ordered variants than
112 for the disordered ferrite. The change of slope of the series of results thus indicates the upper
113 limit of the disordered composition domain for alloys that have been equilibrated.



114

115 Figure 2. Effect of silicon content on the lattice parameter of Fe- α at various temperatures.

116 Data according to Lihl and Ebel [2] after conversion to Ångström. The dashed line represents

117 the upper limit of the disordered Fe-Si ferrite as a function of temperature according to Lihl

118 and Ebel.

119

120 Focusing on the silicon contents lower than that for ordering, i.e. less than 10 at.% as seen in

121 figure 2, the data for 0, 3.7 and 9.5 at.% were selected and replotted in Fig. 3 as function of

122 temperature. The results for 3.7 at.% Si and 9.5 at.% Si show a similar temperature evolution

123 as for pure Fe, which means that the linear expansion does not depend on the silicon content.

124 In the low temperature range, the effect of silicon was estimated as $-6.5 \cdot 10^{-4}$ Å/at.%. A

125 coefficient of $-6.9 \cdot 10^{-4}$ Å/at.% Si was found by Polcarova *et al.* [12] to describe the effect of

126 silicon on the lattice parameter that closely agrees with the present estimate and is definitely

127 at change with the value of $-3.0 \cdot 10^{-4}$ Å/at.% Si suggested by Leslie [13].

128 Equation (1) could thus be complemented to write:

$$129 \quad a_{Fe-\alpha} = 2.8658 + 3.747 \cdot 10^{-5} \cdot T_C + 8.59 \cdot 10^{-9} \cdot (T_C)^2 - 6.5 \cdot 10^{-2} \cdot x_{Si} \quad (2)$$

130 where x_{Si} is the atom fraction of silicon in the iron matrix.

131 The corresponding curves have been plotted in Fig. 3 where it can be seen that most of the

132 experimental values are properly reproduced for temperature lower than 600°C. The

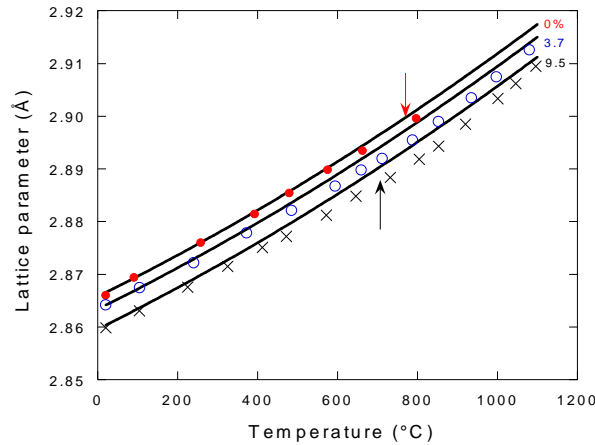
133 disagreement as the temperature increases beyond could well be related to the magnetic

134 transition whose temperature, T_{Curie} , decreases with the silicon content. This temperature can

135 be expressed as $T_{Curie}(K)=1043 \cdot x_{Fe}+504 \cdot x_{Fe} \cdot x_{Si} \cdot (x_{Fe}-x_{Si})$ where x_{Fe} and x_{Si} are the atom

136 fraction of Fe and Si, respectively [14]. The values for pure Fe (770°C) and for the alloy at
137 9.5 at.% Si (706°C) are indicated with the arrows in figure 3.

138



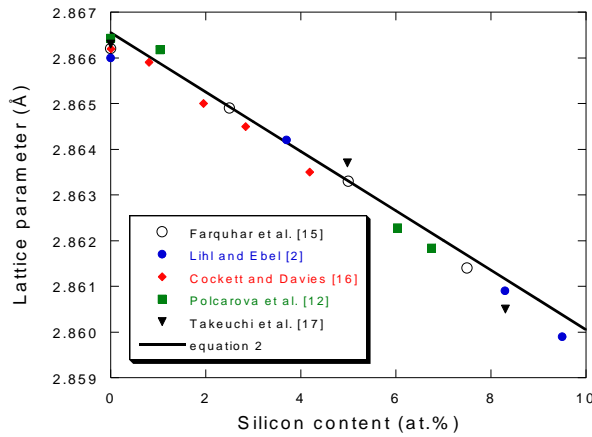
139

140 Figure 3. Effect of temperature on the Fe- α lattice parameter of Fe-Si alloys at 0, 3.7
141 at.% Si (as indicated) according to Lihl and Ebel [2]. The solid lines have been calculated
142 using equation (2). The arrows indicate the Curie temperature for pure Fe and for the alloy at
143 9.5 at.% Si; see text.

144

145 In addition to the results of Lihl and Ebel [2], some other results on Fe-Si alloys at room
146 temperature (set to 20°C) are available from Farquhar *et al.* [15], Cockett et Davis [16],
147 Takeuchi *et al.* [17] and Polcarova *et al.* [12]. They are presented in Fig. 4 and compared to
148 equation (2). The agreement is quite satisfactory though considering the series of results
149 would suggest a slightly non-linear change of the lattice parameter with the silicon content
150 instead of the assumed linear behavior.

151

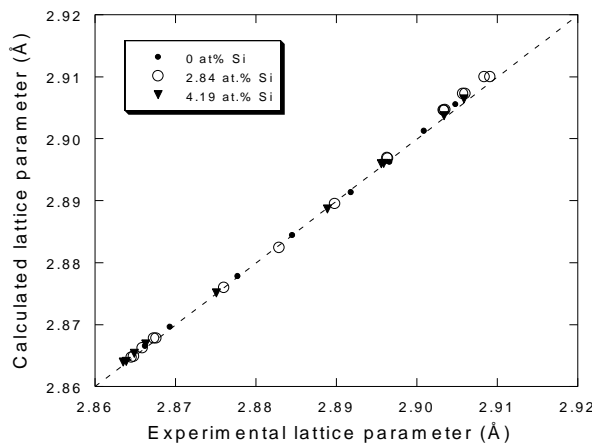


152

153 Figure 4. Effect of silicon content on the ferrite lattice parameter at room temperature:
 154 comparison of experimental data versus equation (2) shown with a solid line. Data from the
 155 references indicated in the caption.

156

157 For further checking the validity of equation (2), we considered the results of Cockett and
 158 Davis [16] who studied Fe-Si alloys from 0.007 to 2.15 wt.% Si at temperature up to 1200°C
 159 in an attempt to better define the limits of the gamma-loop in this system. Fig. 5 compares the
 160 experimental and calculated values for three of their alloys, as indicated in the legend, and for
 161 temperature limited to 1000°C. The agreement appears excellent except for the highest values
 162 at high temperature where predictions slightly overestimate the lattice parameter, probably
 163 because of the magnetic transformation.

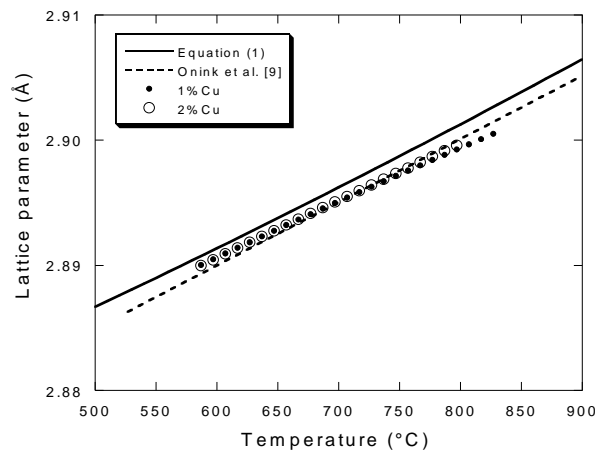


164

165 Figure 5. Experimental lattice parameter of ferrite versus calculated values using equation (2).
 166 Data of three of the alloys investigated by Cockett and Davis [16], nearly pure Fe, an
 167 intermediate one at 1.45 wt.% Si (2.84 at.%) and that with the maximum Si content (2.15
 168 wt.%=4.19 at.%). The dashed line is the bisector.

169

170 The most common other elements present in silicon cast irons at a level that could possibly
171 affect the lattice parameter are Cu, Mn and P. Velthuis *et al.* [18] investigated the effect of Co
172 and Cu on the ferrite to austenite transformation of binary alloys. Using neutron diffraction,
173 they could measure the lattice parameter of both phases on two Fe-Cu alloys, one at 0.8 at.%
174 Cu (denoted 1% Cu) and the second at 1.7 at.% Cu (denoted 2% Cu). Though this second
175 alloy had a composition corresponding to the maximum solubility of Cu in ferrite [19], the
176 authors reported they did not identify Cu precipitation during their experiments. They found
177 that the lattice parameter of ferrite is not really modified by the addition of Cu but proposed
178 an equation describing its variation with temperature for each alloy. These equations are
179 plotted with symbols in Fig. 6 for the investigated temperature domain of 587C (860 K) to
180 827°C (1100 K) where it is seen that they are superimposed on each other. The authors
181 suggested that the negative curvature might be due to the magnetic transformation. Figure 6
182 also shows the lattice parameter for pure Fe according to equation (1) and to Onink *et al.* [9].
183 As in Fig. 1-b, the Onink's equation parallels equation (1) at slightly lower values, while
184 underestimating the lattice parameter in the low temperature domain and overestimating it in
185 the high temperature domain. While Velthuis *et al.* [18] concluded on a relative increase of
186 approximately $0.3 \times 10^{-3} \text{ \AA/at.\% Cu}$ with respect to the lattice parameter of pure Fe for
187 samples with 0.8 and 1.7 at% Cu, it appears reasonable to consider that this element has no
188 effect for the contents encountered in cast irons.



189

190 Figure 6. Comparison of the lattice parameter of ferrite measured by Velthuis *et al.* [18] on
191 Fe-Cu alloys to the lattice parameter of pure Fe as given by equation (1) and by Onink *et al.*
192 [9].

193

194 In the case of Mn solute element, Li *et al.* [20] determined that the lattice parameter of ferrite
195 is linearly dependent on Mn concentration, finding a positive coefficient of $5.43 \cdot 10^{-4}$ Å/at%
196 Mn, which is in good agreement with the value reported by Leslie [13]. On the contrary,
197 phosphorus decreases the lattice parameter by about $9.6 \cdot 10^{-4}$ Å/at.%. [21]. Taking into
198 consideration these values and those relative to carbon and silicon discussed above, the lattice
199 parameter of ferrite is written as:

$$a_{Fe-\alpha} = 2.8658 + 3.747 \cdot 10^{-5} \cdot T_C + 8.59 \cdot 10^{-9} \cdot (T_C)^2 \\ + 8.4 \times 10^{-2} \cdot x_C - 6.5 \cdot 10^{-2} \cdot x_{Si} + 5.43 \cdot 10^{-2} \cdot x_{Mn} - 9.6 \cdot 10^{-2} \cdot x_P \quad (3)$$

201 where x_i is the atom fraction of element i in the single-phase ferritic alloy.

202

203 3. Experimental details and results

204 3.1 Experimental details

205 The investigated alloys have been prepared at the School of Engineering, Jönköping
206 University, using standard practice for Fe-C-Si alloys that will be fully described elsewhere.
207 Their compositions are listed in Table 1, they consist of nine cast irons (A to I) for which
208 foundry returns were used, and three steels (J, K and L) for which purer materials were
209 melted. To these was also added a sample of pure Fe used to check the appropriateness of the
210 defined procedures.

211 A ferritizing annealing was conducted that consisted in a holding under argon at a temperature
212 generally set 10°C below the lower limit of the three-phase field, T_α , whose values are listed
213 in Table 1. The usual holding time was 2 days but the treatment could be repeated in case
214 some pearlite was still present. Alloy J had to be heat-treated for two weeks before any trace
215 of pearlite had disappeared. One sample was then machined out from each material and
216 mechanically polished to mirror finish before being subjected to X-ray diffraction (XRD)
217 analysis in a Bruker D8 Advance equipped with a Cu anticathode and a high-temperature
218 chamber. The XRD measurements were performed using increments of 0.015° in 2θ from 35°
219 to 105° with a scan speed set to 0.5 s per increment. The furnace temperature was controlled
220 by a thermocouple in contact with the heating element, while the actual sample temperature
221 was measured with an S type thermocouple welded to its upper surface. Before starting XRD

222 measurement, the chamber was evacuated and then filled with argon and a constant low flow
 223 of this gas was then maintained to limit sample decarburization and oxidation. The heating
 224 cycle consisted in increasing the furnace temperature by step with 40 minutes holding for
 225 analysis. After XRD measurement at room temperature, the furnace temperature was thus
 226 successively increased to 100°C, 300°C, 500°C, 700°C, 850°C, 1000°C and 1150°C. The last
 227 three temperatures were high enough for the matrix to be partly or fully in the austenite field.
 228 An additional XRD measurement was performed at room temperature after the heating cycle
 229 for comparison purposes.

230

231 Table 1. Chemical composition of the investigated alloys (wt.%) and lower limit of the three-
 232 phase domain, T_{α} , calculated using the TCFE-12 database and the ThermoCalc software
 233 package [22].

Alloy	C	Si	Mn	P	S	Cu	T_{α} (°C)
A	2.95	1.16	0.35	0.017	0.047	0.81	738
B	4.03	1.05	0.38	0.033	0.065	0.83	736
C	2.18	1.19	0.33	0.016	0.056	0.8	741
D	2.1	1.77	0.36	0.02	0.057	0.81	755
E	4.13	2.62	0.343	0.021	0.042	0.718	783
F	2.19	2.55	0.321	0.015	0.059	0.783	780
G	3.915	1.80	0.290	0.026	0.0530	0.804	759
H	2.966	3.94	0.514	0.022	0.0730	0.820	828
I	2.236	4.26	0.684	0.019	0.1130	0.908	837
J	0.995	0.54	0.017	0.010	0.0075	0	748
K	1.03	1.91	0.017	0.022	0.0060	0	779
L	1.1	3.45	0.024	0.027	0.0110	0	829

234

235 The collected XRD data were analyzed to extract the mean lattice parameters by Rietveld
 236 refinement with the Fullprof software. This was done using the first four characteristic
 237 diffraction peaks of ferrite, which are {110}, {200}, {211} and {220}. The error in the lattice
 238 parameter determination was considered as three times the standard deviation reported by the
 239 software, thus obtaining an uncertainty in the order of $3 \cdot \sigma = \pm 0.0007 \text{ \AA}$.

240 Carbon dissolved in ferrite at each temperature was estimated using ThermoCalc and the
 241 TCFE-12 database for all the alloys listed in Table 1. At the highest temperature where ferrite
 242 is stable, it was found that the maximum content of carbon in ferrite would be of the order of
 243 0.15 at.%. According to equation (3), the maximum effect on the ferrite lattice parameter

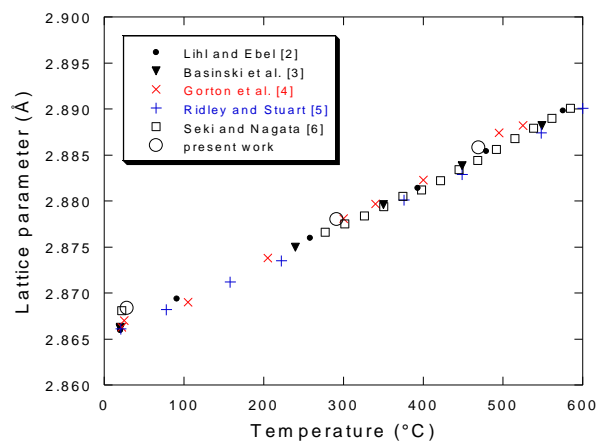
244 would thus be an increase by $1.3 \cdot 10^{-4}$ Å that was considered as negligible owing to the
245 uncertainties.

246 The mean lattice parameters of all samples after the XRD cycle were also determined by
247 using high energy X-ray diffraction (HEXRD) at the P07 beamline of the PETRA III in
248 DESY (Deutsches Elektronen-Synchrotron, Hamburg, Germany). The beamline configuration
249 was a 100 keV monochromatic beam (beam size 0.8×0.8 mm²) corresponding to a wavelength
250 of 0.12074 Å, enabling high penetration depths to be achieved and a large volume to be
251 analyzed in transmission. A 2D-dectector Perkin Elmer XRD 1621 Flat Panel with a
252 resolution of 2048 by 2048 pixels placed at 1513 mm in transmission was employed in order
253 to collect the Debye-Scherrer rings in a diffraction angle 2θ range between 0° and 10.8° with
254 an acquisition time of 5 s. The Debye-Scherrer rings were circularly integrated with Fit2D
255 software to obtain standard 1D diffractogram (I vs 2θ). The error in the lattice parameter due
256 to the resolution detector, in addition to the error inherent in the refinement method, was
257 estimated $\pm 1.10^{-3}$ Å.

258

259 3.2 Results

260 As a check of the XRD procedure, the lattice parameter of a mirror polished sample of pure
261 Fe was measured at room temperature, near 290°C (furnace set at 300°C) and near 470°C
262 (furnace set at 500°C). The present results are reported in Fig. 7 with open circles whose
263 diameter is about $6 \cdot \sigma = 1.4 \cdot 10^{-3}$ Å, together with the data shown in Fig. 1-a for temperature up
264 to 600°C . It is seen that the present results agree with the reported data, being however in the
265 upper range of these values.



266

267 Figure 7. Plot of the present measurements on pure Fe onto the results shown in Fig. 1-a for
268 the temperature range from room temperature to 600°C.

269

270 In order to compare the experimental results on the investigated alloys to prediction, one has
271 to consider the possibility of graphite precipitation within the Fe-rich matrix. Assuming
272 graphite is pure carbon, all substitutional elements entering in the alloy composition will be in
273 solution into the matrix. These elements substitute to iron on the so-called substitutional
274 lattice while carbon if any is located in interstitial sites. The atom fraction of a substitutional
275 element i , x_i , should thus be referred to the sum of the atom fraction of all substitutional
276 elements. Excluding low level elements, this sum includes Fe, Si, Cu, Mn and P, and writes
277 $S = x_{Fe} + x_{Si} + x_{Cu} + x_{Mn} + x_P$ that will be lower than one.

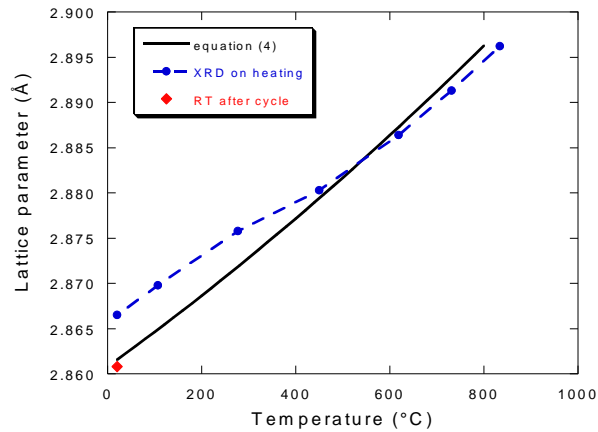
278 Accordingly, equation (3) should be modified as following:

$$a_{Fe-\alpha} = 2.8658 + 3.747 \cdot 10^{-5} \cdot T_C + 8.59 \cdot 10^{-9} \cdot (T_C)^2$$

279 $+ 0.084 \cdot x_C^\alpha + \frac{1}{S} \cdot (-0.065 \cdot x_{Si} + 0.0543 \cdot x_{Mn} - 0.096 \cdot x_P)$ (4)

280 where x_C^α is the atom fraction of carbon dissolved in ferrite and copper does not appear in the
281 brackets because having no influence on the lattice parameter. If there are no other interstitial
282 element than carbon and if the amount of carbon dissolved in ferrite is negligible, note that
283 $S = 1 - x_C$, where x_C is the atom fraction of carbon in the alloy.

284 The lattice parameter from XRD results for each alloy were compared to the prediction from
285 equation (4) as illustrated in Fig. 8 in the case of alloy I. It is seen that the experimental lattice
286 parameter increases with temperature as expected, but being significantly above the
287 predictions for temperatures up to 500°C. Also, it is noticed that the dilatation coefficient
288 decreases strongly between 300°C and 500°C, and that above this temperature the predictions
289 are in quite close agreement with the measurements. The temperature range of 300-500°C is
290 not compatible with the magnetic transformation that occurs above 650°C in Fe-Si ferrite.
291 Moreover, it was observed that the value at room temperature after the heating cycle
292 (diamond in the figure) was much lower than the initial value, and in perfect agreement with
293 the prediction.



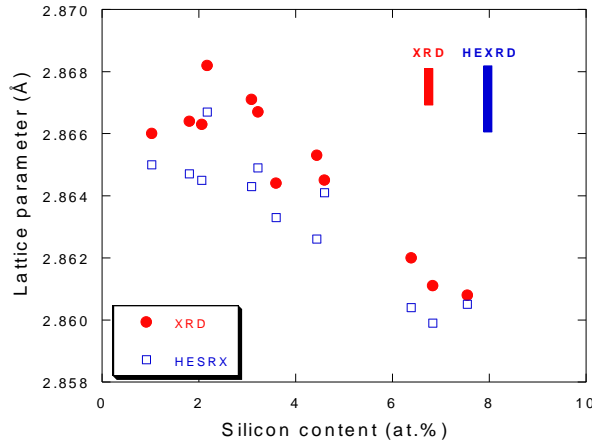
294

295 Figure 8. Evolution of the Fe- α lattice parameter of alloy I upon heating (symbols along the
 296 dashed line) and room temperature value after cooling down (RT after cycle). The solid line is
 297 according to equation (4).

298

299 The behavior illustrated in Fig. 8 was observed on all investigated alloys. Considering poor
 300 grain statistics with laboratory X-rays or partial ordering/disordering of the Fe-Si ferritic
 301 matrix could not explain the discrepancy. In fact, additional experiments described in
 302 appendix A demonstrated that the measurements were highly sensitive to the sample polishing
 303 procedure. Mechanical polishing as used in the present investigation should have generated
 304 strains that then disappeared when heating the sample above 500°C, thus explaining the
 305 change in the lattice parameter at room temperature after the thermal cycle.

306 Synchrotron measurements are not sensitive to such surface defects and all samples after the
 307 XRD run were tested with the synchrotron at room temperature. The lattice parameter values
 308 thus obtained are plotted in Fig. 9 where are shown also the XRD values obtained after
 309 cooling back to room temperature. The ranking according to the silicon content of the alloy
 310 was used to ease reading but could not be strictly compared to the plot in Fig. 4 because the
 311 actual amount of silicon in the substitutional lattice depends on the amount in carbon and in
 312 other elements of the alloy. It is seen that the HEXRD values are generally slightly lower than
 313 the XRD values but that the overall agreement is quite good owing to the indicated
 314 uncertainties.



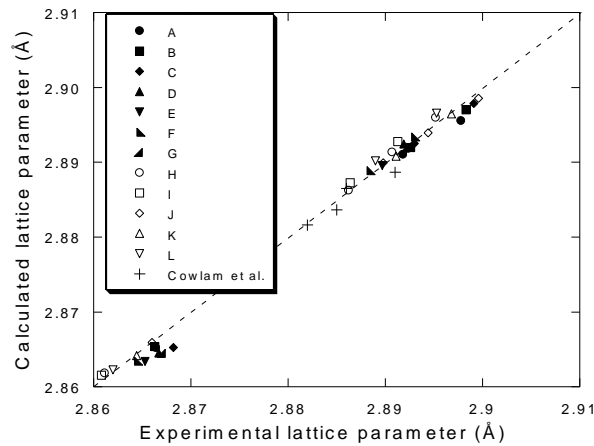
315

316 Figure 9. Evolution with the silicon content of the ferrite lattice parameter as measured by
 317 XRD and by HEXRD after the XRD cycle. The vertical lines indicate the expected accuracy
 318 on the lattice parameter, namely $(\pm 3\sigma)$ for XRD and $\pm 1.10^{-3} \text{ \AA}$ for HEXRD measurements.

319

320 The results in Fig. 8 led to disregard XRD data obtained upon heating from room temperature
 321 to 500°C. A comparison of all experimental values against the prediction with equation (4)
 322 appears in Fig. 10 where the values in the lower left corner were obtained after cooling back
 323 to room temperature. Also, the high-temperature results where both ferrite and austenite were
 324 recorded have not been considered because the phases may strain each other during the
 325 transformation [18].

326 Very few other results are available from literature. Those of Huyan *et al.* [23] could not be
 327 considered because no detail was given on the composition of the investigated alloys apart for
 328 the silicon content. Neutron diffraction was performed by Cowlam *et al.* [24] on a Fe-C-Si
 329 alloy (1.14% C, 2.03% Si and 0.24% Mn, per weight) tested between 490°C and 597°C and
 330 the results are also shown in Fig. 10. On the whole, the agreement between prediction with
 331 equation (4) and experimental XRD values appear quite satisfactory in Fig. 10. It is thus
 332 surprising that the effect of the magnetic transformation does not show up, which could mean
 333 that it is smoothed by alloying.



334

335 Figure 10. Experimental XRD values of the lattice parameter of ferrite versus values predicted
 336 with equation (4). The dashed lines are the bisector. Values reported by Cowlam *et al.* [24]
 337 have been included.

338

339 **Conclusion**

340 The review of literature data allowed deriving an expression for the lattice parameter of ferrite
 341 based on that for pure iron to which were added the individual effects of carbon, silicon,
 342 manganese and phosphorus, while it appeared that copper might not have any effect. The
 343 initial expression thus obtained is valid for a homogeneous single-phase material and was
 344 corrected to account for the presence of graphite in cast irons.

345 The lattice parameter of a series of 12 alloys with carbon between 1.0 and 4.1 wt.%, silicon
 346 between 0.5 and 4.3, up to 0.7 wt.% Mn and 0.9 wt.% Cu has been measured by XRD from
 347 room temperature to temperature as high as 1150°C but only records without austenite were
 348 considered. It was quite unexpected that the mirror polish used to prepare the sample should
 349 lead to such extensive alteration of the sample surface, which could be due to the softness of
 350 the ferrite phase. Use of electrolytic polishing would have solved the issue that was realized
 351 after the whole set of XRD results had been recorded. Room temperature HEXRD was thus
 352 carried out that are free of any surface effect such as oxidation, decarburization or mechanical
 353 deformation. Valid room temperature measurements and the XRD values obtained at
 354 temperature higher than 500°C were compared successfully with predictions. The effect of the
 355 magnetic transformation that is so evident with pure Fe seems to be smoothed by alloying,
 356 though this conclusion needs further confirmation.

357

358 **Acknowledgements**

359 Thanks are due to A. Dioszegi, B. Domeij and Lucian-Vasile Diaconu for providing the alloys
360 for this work. The authors also acknowledge people at the accelerator DESY (Hamburg,
361 Germany), a member of the Helmholtz Association HGF, for the provision of experimental
362 facilities. Parts of this research were carried out at PETRA III and we would like to thank E.
363 Maawad for assistance in using the P07 beamline. Beam-time was allocated for proposal I-
364 20230170 EC.

365

366 **No conflict section**

367 The authors declare they have no conflict of interest

368

369 **References**

370 [1] A. Jablonka, K. Harste and K. Schwerdtfeger: *Steel Research*, 1991, vol. 62, pp. 24-33.

371 [2] F. Lihl and H. Ebel: *Arch. Eisenhüttenwesen*, 1961, vol. 32, pp. 489-491.

372 [3] Z.S. Basinski, W. Hume-Rothery and A.L Sutton: *Proceedings of the Royal Society of*
373 *London. Series A, Mathematical and Physical Sciences*, 1955, vol. 229, No. 1179, pp. 459-
374 467.

375 [4] A.T. Gorton, G. Bitsianes and T.L. Joseph: *Transactions of the Metallurgical Transactions*
376 *of AIME*, 1965, vol. 233, pp. 1519-1525.

377 [5] N. Ridley and H. Stuart: *Brit. J. Appl. Phys. (J. Phys. D) ser. 2*, 1968, 1, pp. 1291-1295.

378 [6] I. Seki and K. Nagata: *ISIJ International*, 2005, vol. 45, pp. 1789-1794.

379 [7] W. Bragg and E. Armstrong-Wood: *J. Am. Chem. Soc.*, 1947, vol. 69, p. 2919.

380 [8] S.-J. Lee and Y.-K. Lee: *Scripta Mater.*, 2005, vol. 52, pp. 973-976.

381 [9] M. Onink, C.M. Brakman, F.D. Tichelard *et al.*: *Scripta Metal. Mater.*, 1993, vol. 29, pp.
382 1011-1016.

383 [10] E.J. Fasiska and H. Wagenblast: *Trans. Metall. Soc. AIME*, 1967, vol. 239, pp. 1818-
384 1820

385 [11] V. Ye. Polishchuk and Ya. P. Selisskiy: *Fiz. Metal. Metalloved.*, 1970, vol. 29, pp. 1101-
386 1104.

387 [12] M. Polcarova, K. Godwod, J. Bak-Misiuk, S. Kadeckova and J. Bradler: *Physica status*
388 *solidi (a)*, 1988, vol. 106, pp. 17-23.

389 [13] W.C. Leslie: *Metallurgical Transactions*, 1972, vol. 3, pp. 5-26.

390 [14] J. Lacaze and B. Sundman: *Metall. Trans. A*, 1991, vol. 22A, pp. 2211-2223.

- 391 [15] M. C. Farquhar, H. Lipson and A. R. Weill: *J. Iron Steel Inst.*, 1945, vol. 152, pp. 457-
392 472.
- 393 [16] G.H. Cockett and C.D. Davis: *J. Iron Steel Inst.*, 1963, vol. 201, pp. 110-115.
- 394 [17] S. Takeuchi, H. Yoshida and T. Taoka: *Trans. of the Japan Institute of Metals*, 1968, vol.
395 9, pp. 715-719.
- 396 [18] S.G.E. Te Velthuis, J.H. Root, J. Sietsma, H. Th. Rekveldt and S. Van Der Zwaag: *Acta*
397 *Materialia*, 1998, vol. 46, pp. 5223-5228.
- 398 [19] Qing Chen and Zhanpeng Jin: *Metall. Mater. Trans. A*, 1995, 26A, pp. 417-426.
- 399 [20] C. Li, F. Sommer and E.J. Mittemeijer: *Materials Science and Engineering*, 2002, vol.
400 A325, pp. 307-319.
- 401 [21] H. Hattendorf, A.R. Büchner and G. Inden: *Steel Research*, 1988, vol. 59, pp. 279-280.
- 402 [22] <https://thermocalc.com/products/databases/>
- 403 [23] F. Huyan, R. Larker, P. Rubin and P. Hedström: *ISIJ International*, 2014, vol. 54, pp.
404 248-250.
- 405 [24] N. Cowlam, G. E. Bacon, L. Gillott and D. H. Kirkwood: *Acta Metallurgica*, 1981, vol.
406 29, pp. 651-660.
- 407 [25] M. Vashista and S. Paul: *Philosophical Magazine*, 2012, vol. 92, pp. 4194-4204.
- 408 [26] F. Jiang, K. Hirata, T. Masumara, T. Tsuchiyama and S. Takaki: *ISIJ International*,
409 2018, vol. 58, pp. 376-378.
- 410 [27] R. Gadallah, S. Tsutsumi, Y. Aoki and H. Fujii: *Journal of Manufacturing Processes*,
411 2021, vol. 64, pp. 1223-1234.

412

413 **Appendix A**

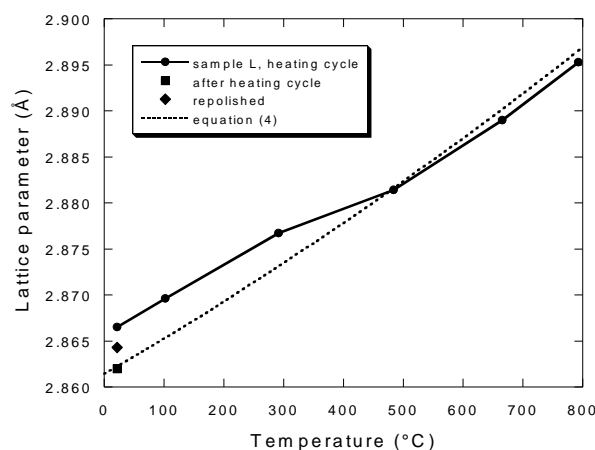
414 Considering poor grain statistics with laboratory X-rays or partial ordering/disordering of the
 415 matrix could not explain the discrepancies observed in the room temperature lattice
 416 parameters before and after the XRD heating cycle. This discrepancy is again illustrated in
 417 Fig. A1 in the case of alloy L. It was then considered that strains developed during polishing
 418 could be the reason for this. The sample corresponding to alloy L was again submitted to
 419 mechanical polishing after the XRD cycle and the lattice parameter was again measured in
 420 this condition. The results at room temperature in Fig. A1 and table AI show that the value of
 421 the lattice parameter decreased by 0.004 Å from before to after the XRD cycle, and increased
 422 by 0.002 Å by polishing again the cycled XRD sample.

423

424 Table AI. Change in the room temperature lattice parameter obtained by XRD for Sample L
 425 before and after the heating cycle, taking into consideration the effect of polishing.

Condition of the sample	Lattice parameter (Å)
Before heating cycle (polished)	2.8665
After heating cycle (not polished)	2.8620
Repolished after heating cycle	2.8643

426

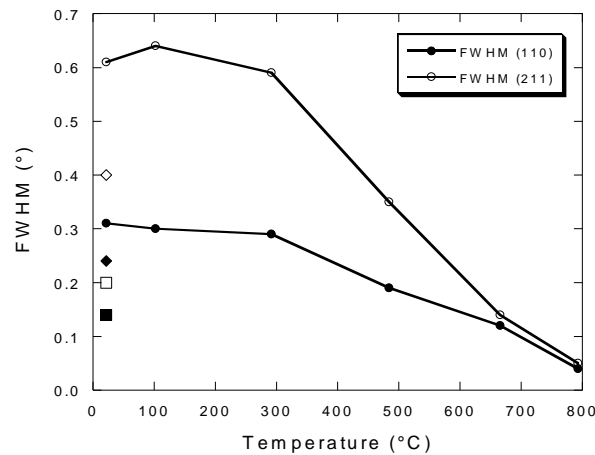


427

428 Figure A1. Evolution of the lattice parameter of alloy L upon heating (disks) and room
 429 temperature values after cooling down in the non-polished (square) and repolished (diamond)
 430 condition.

431

432 The effect of plastic deformation associated with polishing on XRD records has been known
 433 since a long time and is still regularly reported. Quite recently again, Vashista and Paul [25],
 434 Jiang *et al.* [26], and Gadallah *et al.* [27] noticed a close relation between the full width at half
 435 maximum (FWHM) of X-ray peaks with the strain or stress state, and Jiang *et al.* also
 436 emphasized the possible errors this implies on XRD data. All records of the XRD samples
 437 investigated during this work were checked and showed high FWHM at temperature lower
 438 than 400°C when compared to higher temperature, as illustrated in Fig. A2 for alloy L. This
 439 effect was found more prominent for the (211) peak than for the (110) peak. For A, B and K
 440 alloys, it was observed that the FWHM increased again at high temperature after going
 441 through a minimum at temperature between 600°C and 700°C, which could well be related to
 442 the fact that ferrite coexisted with austenite in these samples for temperature higher than
 443 800°C.



444
 445 Figure A2. Evolution with temperature of the FWHM of (110) and (211) XRD peaks for
 446 sample L. Solid and empty symbols are for (110) and (211) peaks respectively, circles for the
 447 heating cycle, squares for the values after the cycle and diamonds for repolished sample.

448
 449 According to these observations, it was concluded that the discrepancies found in the room
 450 temperature lattice parameter of ferrite are mainly due to a high sensitivity to the polishing
 451 procedure. This effect vanishes as the sample temperature goes beyond 500°C, and does not
 452 appear again after cooling back to room temperature. Check of sample type and preparation
 453 used in literature works reporting room temperature lattice parameter for pure Fe showed
 454 most of them used powder or fillings that had been stress relieved before experiments.